HAL
archives-ouvertes.fr

Internal waves and boundary layers in a density-stratified fluid

Bruno Voisin, Sylvain Joubaud, Thierry Dauxois

▶ To cite this version:

Bruno Voisin, Sylvain Joubaud, Thierry Dauxois. Internal waves and boundary layers in a density-stratified fluid. 23rd International Conference on Theoretical and Applied Mechanics, Aug 2012, Beijing, China. pp.FM16-013, 2012. <hal-00744304>

HAL Id: hal-00744304
https://hal.archives-ouvertes.fr/hal-00744304

Submitted on 22 Oct 2012

INTERNAL WAVES AND BOUNDARY LAYERS IN A DENSITY-STRATIFIED FLUID

Bruno Voisin*a), Sylvain Joubaud** & Thierry Dauxois**

*Laboratoire des Écoulements Géophysiques et Industriels, CNRS and Université de Grenoble,
38041 Grenoble, France
**Laboratoire de Physique, CNRS and ENS de Lyon, 69007 Lyon, France

Summary Various theories of internal gravity wave generation by the broadside oscillations of a horizontal circular disk are reviewed and compared with existing low-resolution conductimetric measurements and new high-resolution PIV measurements.

MOTIVATION

Internal tides, generated in the density-stratified ocean by the oscillation of the barotropic tide over bottom topography, play a crucial role in the energy balance of the Earth–Moon system [1]. This has led to a recent revival of the classical topic of internal gravity wave generation by oscillating bodies. Wave energy dissipates owing to wave breaking and sub- and superharmonic excitation, at regions where the wave rays either intersect each other, reflect at the bottom or are tangent to the topography [2]. Accordingly, accurate modelling of the bottom boundary condition is determinant. However, all analytical models to date consider idealized free-slip boundaries instead of the actual no-slip boundaries, except for a recent study of the oscillating circular disk [3]. We specialize to this problem, review the possible theoretical approaches and compare their outcome with existing experimental data and with a new and improved set of data.

THEORY

A horizontal circular disk of radius a oscillates vertically at the frequency ω with velocity $w_0 e^{-i\omega t}$ in a uniformly stratified fluid of buoyancy frequency N with $\omega < N$, as shown in Figure 1. In cylindrical coordinates (r, φ, z) non-dimensionalized as $(R, \varphi, Z) = (r, \varphi, z)/a$, with upward vertical z-axis, the inviscid solutions of [4, 5, 6] are all equivalent to the integral representation, for the vertical velocity w non-dimensionalized as $W = w/w_0$,

$$W = \frac{2}{\pi} \exp(-i\omega t) \int_0^\infty K j_1(K) J_0(KR) \exp(-iK|Z| \tan\theta) \, dK, \tag{1}$$

with $\theta = \arccos(\omega/N)$ the angle of propagation of the waves to the vertical and J_0 and j_1 cylindrical and spherical Bessel functions, respectively.
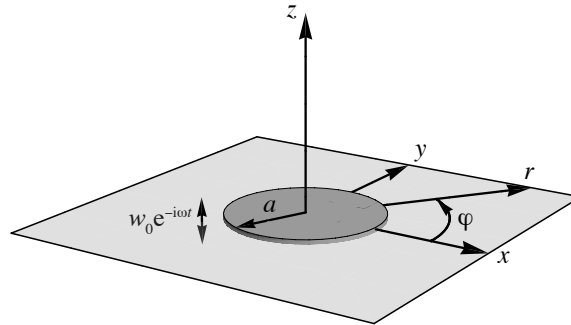
Figure 1. Oscillating disk geometry.

Kinematic viscosity ν affects the waves according to the Stokes number $S^2 = \omega a^2/\nu$. For large S^2, it is generally believed that only wave propagation is affected while generation remains inviscid [7]. Hence, with free-slip forcing and viscous wave attenuation according to [8, §4.10] corrected in [9] for near-field effects, the velocity becomes

$$W = \frac{2}{\pi} \exp(-i\omega t) \int_0^\infty K j_1(K) J_0(KR) \exp(-iK|Z| \tan\theta) \exp\left(-\frac{K^3|Z|}{2S^2 \sin\theta \cos^3\theta}\right) dK. \tag{2}$$

For arbitrary S^2 hence no-slip forcing, [10] reduced artificially the problem to a Dirichlet one by replacing the actual disk by one oscillating through an aperture in an infinite fixed plate, whereas [3] solved the proper mixed problem by Tranter's method. We retain the latter. A combination of two terms follows,

$$W = \exp(-i\omega t) \int_0^\infty A(K) J_0(KR) \left[\frac{\exp(-\Lambda_1|Z|)}{\Lambda_1} - \frac{\exp(-\Lambda_2|Z|)}{\Lambda_2}\right] dK, \tag{3}$$

---

a)Corresponding author. E-mail: bruno.voisin@legi.grenoble-inp.fr.

namely the waves themselves with complex attenuation factor Λ_1 and a boundary layer with attenuation factor Λ_2, where

$$\left.\begin{array}{c}\Lambda_1^2\\\Lambda_2^2\end{array}\right\} = K^2 - \mathrm{i}\frac{S^2}{2} \pm \mathrm{i}\frac{S^2}{2}\left(1 + 4\mathrm{i}\frac{K^2}{S^2\cos^2\theta}\right)^{1/2}, \tag{4}$$

and $\mathrm{Re}\,\Lambda_{1,2} > 0$. The amplitude $A(K)$ is a Neumann series of spherical Bessel functions,

$$A(K) = \frac{K^3}{\Lambda_2^2 - \Lambda_1^2}\sum_{m=0}^{\infty} a_m j_{2m}(K), \tag{5}$$

with coefficients satisfying an infinite linear system solved by truncation,

$$\sum_{m=0}^{\infty} a_m \int_0^{\infty} \frac{K^2 j_{2l}(K) j_{2m}(K)}{[2K^2 - \mathrm{i}S^2 + 2K(K^2 + \mathrm{i}S^2\tan^2\theta)^{1/2}]^{1/2}(K^2 + \mathrm{i}S^2\tan^2\theta)^{1/2}}\,\mathrm{d}K = \delta_{l0}. \tag{6}$$

As $S^2 \to \infty$ the boundary layer becomes negligible except close to the disk and the waves reduce to (2).

EXPERIMENT

We assess the relative merits of these theories by comparison with experiment in Figure 2. The only data to date are conductimetric measurements for a large disk at high $S^2 = 1000$ and a small disk at lower $S^2 = 210$ [10]. Only the viscous theories (2) and (3)–(6) account for the asymmetry of the profile for the large disk in Figure 2(a), but poor data sampling prohibits more definite conclusions to be drawn. To overcome these limitations, new experiments were performed at ENS de Lyon using Particle Image Velocimetry at high resolution. Comparison in Figure 2(c) for a small disk at $S^2 = 250$ shows excellent agreement about the shape of the profile for the two theories, but some disagreement persists about the amplitude, attributed to the small but finite thickness of the experimental disk (ensuring its rigidity).
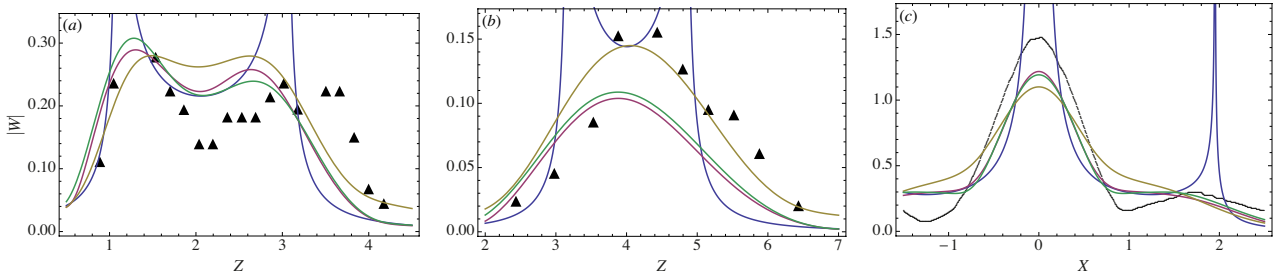
Figure 2. Velocity envelope along a vertical line $R = \mathrm{const}$ for (a) the large disk of $S^2 = 1000$ and (b) the small disk of $S^2 = 210$ in the experiments of [10], and along the horizontal line ($Y = 0, Z = 1$) for (c) the disk of $S^2 = 250$ in the present experiments. The black markers represent the experimental data: 18 and 10 big triangles in (a) and (b), respectively, and 841 small circles in (c). The lines represent the theoretical predictions: (1) in blue, (2) in red, from [10] in olive green and (3)–(6) in apple green.

In order to discriminate between the large-S^2 theory (2) and the finite-S^2 theory (3)–(6), larger values of S^2 must be considered. At $S^2 = 1000$, the two theories still exhibit a small discrepancy in Figure 2(a). The boundary layer term, at least 10^6 times smaller that the wave term, is not involved. Closer investigation shows that it is only for $S^2 = 0(10^6)$ that the large-S^2 limit is actually reached, prohibiting the use of free-slip boundaries at any smaller S^2.

CONCLUSION

Based on the example of the oscillating disk, we have shown the classical approximation of free-slip forcing at an internal wave generator to apply only for extremely large S^2, and consideration of no-slip forcing to be required otherwise.

References

[1] Garrett C., *Science* **301**:1858–1859, 2003; Garrett C., Kunze E., *Annu. Rev. Fluid Mech.* **39**:57–87, 2007.
[2] Korobov A.S., Lamb K.G., *J. Fluid Mech.* **611**:61–95, 2008.
[3] Davis A.M.J., Llewellyn Smith S.G., *J. Fluid Mech.* **656**:342–359, 2010.
[4] Sarma L.V.K.V., Krishna D.V., *Zastosow. Matem.* **13**:109–121, 1972.
[5] Gabov S.A., Pletner Yu.D., *USSR Comput. Maths Math. Phys.* **28**(1):41–47, 1988.
[6] Martin P.A., Llewellyn Smith S.G., *Proc. R. Soc.* A **467**:3406–3423, 2011.
[7] Hurley D.G., Keady G., *J. Fluid Mech.* **351**:119–138, 1997.
[8] Lighthill J.: Waves in Fluids. Cambridge University Press, 1978.
[9] Voisin B., *J. Fluid Mech.* **496**:243–293, 2003; Voisin B., Ermanyuk E.V., Flór J.-B., *J. Fluid Mech.* **666**:308–357, 2011.
[10] Bardakov R.N., Vasil'ev A.Yu., Chashechkin Yu.D., *Fluid Dyn.* **42**:612–626, 2007.